

# Molecular classification of head and neck squamous cell carcinomas using patterns of gene expression

Christine H. Chung,<sup>1,2</sup> Joel S. Parker,<sup>3</sup> Gamze Karaca,<sup>3,4</sup> Junyuan Wu,<sup>3,4</sup> William K. Funkhouser,<sup>3,5</sup> Dominic Moore,<sup>3,6</sup> Dale Butterfoss,<sup>3,4</sup> Dong Xiang,<sup>3</sup> Adam Zanation,<sup>7</sup> Xiaoying Yin,<sup>7</sup> William W. Shockley,<sup>7</sup> Mark C. Weissler,<sup>7</sup> Lynn G. Dressler,<sup>8</sup> Carol G. Shores,<sup>7</sup> Wendell G. Yarbrough,<sup>2,9,10</sup> and Charles M. Perou<sup>3,4,5,\*</sup>

<sup>1</sup>Division of Hematology/Oncology, Department of Medicine

<sup>2</sup>Vanderbilt-Ingram Cancer Center

Vanderbilt University School of Medicine, 2220 Pierce Avenue, 777 Preston Research Building, Nashville, Tennessee 37232

<sup>3</sup>Lineberger Comprehensive Cancer Center

<sup>4</sup>Department of Genetics

<sup>5</sup>Department of Pathology and Laboratory Medicine

<sup>6</sup>Department of Biostatistics

<sup>7</sup>Department of Otolaryngology/Head and Neck Surgery

<sup>8</sup>Department of Medicine

University of North Carolina at Chapel Hill, Chapel Hill, North Carolina 27599

<sup>9</sup>Department of Otolaryngology

<sup>10</sup>Department of Cancer Biology

Vanderbilt University, S-2100 Medical Center North, Nashville, Tennessee 37232

\*Correspondence: cperou@med.unc.edu

## Summary

**The prognostication of head and neck squamous cell carcinoma (HNSCC) is largely based upon the tumor size and location and the presence of lymph node metastases. Here we show that gene expression patterns from 60 HNSCC samples assayed on cDNA microarrays allowed categorization of these tumors into four distinct subtypes. These subtypes showed statistically significant differences in recurrence-free survival and included a subtype with a possible EGFR-pathway signature, a mesenchymal-enriched subtype, a normal epithelium-like subtype, and a subtype with high levels of antioxidant enzymes. Supervised analyses to predict lymph node metastasis status were approximately 80% accurate when tumor subsite and pathological node status were considered simultaneously. This work represents an important step toward the identification of clinically significant biomarkers for HNSCC.**

## Introduction

Tumors of head and neck, which include the upper aerodigestive tract (oral cavity, oropharynx, hypopharynx, and larynx), account for over 40,000 cases of cancer per year in the US (Jemal et al., 2002; Landis et al., 1999). The most common histology of head and neck tumor is squamous cell carcinoma. The main prognostic variables of head and neck squamous cell carcinoma (HNSCC) are the location and size of the tumor, the presence of distant metastasis, and the presence of cervical lymph node (LN) metastasis (Andersen et al., 1994; Sessions et al., 2002). About 40%–50% of patients with advanced disease (Stage III and IV) recur, and approximately 80% of recurrences occur

within the first two years (Jones et al., 1992; Takes et al., 1997). Most of the clinical decisions regarding therapy are commonly based upon clinical staging, which relies on nodal status and tumor size. No biomarkers analogous to the estrogen receptor or HER2 in breast cancers, or c-KIT in gastrointestinal stromal tumors, exist for HNSCC patients, suggesting that genomic profiling studies may be useful for identifying new biomarkers with prognostic or predictive value.

Gene expression analyses have proven to be a useful tool for the classification of human solid tumors arising from a single organ site (Garber et al., 2001; Huang et al., 2003; Perou et al., 2000) or from different sites (Ramaswamy et al., 2001). These organ site-specific studies have typically subclassified tumors

## SIGNIFICANCE

**Despite the aggressive multimodality treatment of HNSCC patients with surgery, chemotherapy, and radiation therapy, approximately 40%–50% of patients with advanced disease recur. To date, there are no reliable biomarkers to predict who will have poor clinical outcome. In this study, we identified four distinct subtypes of HNSCC tumors based upon patterns of gene expression that showed clinically distinct behaviors and which showed different patterns of EGFR pathway activation, even within EGFR-expressing tumors. This finding could prove important for the selection of patients for treatment with EGFR inhibitors. In addition, we identified an expression signature that could predict the presence of lymph node metastases using the primary tumor from the time of diagnosis. If these data can be validated on independent cohorts, then these gene expression patterns will provide valuable information that can be used to assist in treatment decisions for HNSCC.**

into relatively homogenous groups based upon their gene expression patterns and have shown that these groupings can predict clinical outcomes (Alizadeh et al., 2000; Bhattacharjee et al., 2001; Dhanasekaran et al., 2001; Garber et al., 2001; Sorlie et al., 2001). Furthermore, lymph node metastasis status can sometimes be predicted from the gene expression patterns of primary tumors (Huang et al., 2003; MacDonald et al., 2001), which could spare many patients from unnecessary lymph node dissections. Here we have analyzed the gene expression patterns of 60 HNSCC tumors and identified distinct subtypes of HNSCC with different clinical outcomes. Many of the patterns identified in this study have also been seen in other tumor studies focused on breast and lung carcinomas (Garber et al., 2001; Perou et al., 2000), and some have been seen in other airway epithelial studies (Ha et al., 2003; Hackett et al., 2003). In addition, we were able to identify patterns of expression that could predict the presence of LN metastases in HNSCC tumors using profiles that have been shown to be involved in metastasis predictions in breast cancers (Huang et al., 2003; van 't Veer et al., 2002). These common patterns suggest that tumors from different sites may share similar cells of origin or common pathways for tumorigenesis and metastasis.

## Results

### Class discovery for HNSCC

Sixty HNSCC samples were assayed using Agilent cDNA microarrays containing 12,814 human genes. Patient demographics are presented in Table 1 and the individual patient/tumor characteristics are presented in Supplemental Table S1 (see <http://www.cancer.org/cgi/content/full/5/5/489/DC1>; <http://dragon.med.unc.edu/pubsup/HN/>). To characterize the diversity of HNSCC tumors, we performed an "intrinsic" analysis and identified 582 cDNA clones whose expression optimally reflected patterns of expression intrinsic to the tumors (Bhattacharjee et al., 2001; Garber et al., 2001; Perou et al., 2000; Sorlie et al., 2003). Using this gene set, we analyzed 74 samples in a two-way average-linkage hierarchical clustering analysis (Figure 1 and see Supplemental Figure S1 for the complete cluster diagram). The cluster analysis identified at least four groups/subtypes within the 60 tumors based upon the sample associated cluster dendrogram (Figure 1B), which were designated as Groups 1 through 4 based on the dendrogram branches. As expected, all 11 intrinsic pairs used for this analysis were closely grouped together on terminal branches of the cluster associated sample dendrogram.

The subtype of tumors on the far left (Group 1, red dendrogram branch) showed the highest expression of the genes in Figures 1C and 1E. Contained within Figure 1C were the genes for Bullous Pemphigoid Antigen 1, P-Cadherin, Laminin  $\gamma$  2, Collagen XVII- $\alpha$ , and two other Laminin subunits ( $\alpha$  3 and  $\beta$  2). These first four genes are also present in the gene set that define the breast "basal-like" tumor subtype (Perou et al., 2000), which is a group of breast tumors that display basal-epithelial cell characteristics and show poor patient outcomes (Sorlie et al., 2001, 2003). The Figures 1C and 1E patterns also share significant expression similarity with the lung squamous carcinoma pattern of Garber et al. (2001), which showed high expression of Bullous Pemphigoid Antigen 1, Collagen XVII- $\alpha$ , FGF-BP, and Kallikrein 10. The other defining gene set for this tumor

**Table 1.** Overall clinical characteristics of HNSCC patients

Age	
Median (range)	56 yr (30–77)
≤40	4 (7%)
>40	56 (93%)
Sex	
Male	53 (88%)
Female	7 (12%)
Ethnicity	
White	37 (62%)
Black	18 (30%)
Others	5 (8%)
Tobacco use	
Yes	58 (97%)
No	2 (3%)
Alcohol use	
Yes	51 (85%)
No	9 (15%)
Tumor sites in head and neck	
Oral cavity	15 (25%)
Oropharynx	14 (23%)
Hypopharynx	7 (12%)
Larynx	24 (40%)
Clinical Stage	
I-II	11 (18%)
III	14 (23%)
IV	35 (58%)
Clinical cervical lymph node metastasis	
Positive	33 (55%)
Negative	27 (45%)
Pathological cervical lymph node metastasis	
Positive	26 (43%)
Negative	14 (23%)
Unknown	20 (33%)
Pathological differentiation	
Well	10 (17%)
Moderate	39 (65%)
Poor	11 (18%)

subtype (Figure 1E) contained genes involved in desmosome function (Desmocollin 2, Desmoglein 3, and Cytokeratin 14) and a homeobox gene that has been implicated in controlling the expression of cell adhesion molecules (BarH-like homeobox 2) (Edelman et al., 2000). Immunohistochemical (IHC) analysis of these tumors for gene products from Figure 1E showed that all 16 tested had high expression of Cytokeratin 14 and 14/16 were positive for Desmoglein 3 (Figures 2E and 2F), while the other tumor subtypes showed much less consistent expression of these proteins (Figure 2G).

It is well known that the epidermal growth factor receptor (EGFR) pathway is important for HNSCC (Endo et al., 2000; Grandis, 1998). The gene set in Figure 1E contained at least three genes from this pathway including TGF $\alpha$ , FGF-BP, and MMK6. TGF $\alpha$  is a ligand for EGFR and a critical activator of the EGFR pathway in HNSCC (Endo et al., 2000; Grandis, 1998). FGF-BP is a promoter of angiogenesis that is induced by EGF

in vitro and induced by the ectopic expression of MMK6, which is a MAP kinase kinase that can be downstream of EGFR (Harris et al., 2000). Among the 60 tumors that were analyzed by microarray, 56 were also analyzed by immunohistochemistry (IHC) for the presence of EGFR and for the Tyr-1173 phosphorylated form of EGFR (see Supplemental Table S1 at <http://www.cancercell.org/cgi/content/full/5/5/489/DC1>). Of these 56 tumors, 54 were positive for EGFR expression and 35/54 of the EGFR-expressing tumors were also positive for P-Tyr-1173-EGFR. Among the Group 1 tumors, all tested were IHC positive for EGFR and a high percentage (15/19, 79%) were positive for P-Tyr-1173-EGFR (50% of Group 2, 75% of Group 3, and 38% of Group 4 tumors were positive for P-Tyr-1173-EGFR). These data suggest that EGFR signaling is typically active in Group 1 and 3 tumors. These data also show that not all EGFR+ tumors have activated EGFR, which is likely influenced by the presence of ligands like TGF $\alpha$ .

The subtype of tumors on the center dendrogram branch (Group 2, blue branch) showed the highest expression of the genes in Figure 1F. Many of these genes are typically produced by fibroblasts/mesenchymal cells including Vimentin, Syndecan 2, Lysyl-oxidase, and four Collagen subunits (Perou et al., 2000). This subtype also tended to show low expression of the gene sets that defined the other subtypes, namely the clusters in Figures 1C, 1D, and especially 1E (Figure 2G). IHC for Vimentin across our cohort of tumors identified eight tumors where the malignant cells were positive for Vimentin staining; of these eight tumors, four (4/19, 21%) were in Group 1 and four (4/12, 33%) were in Group 2 (Figure 2H). In addition, 7/14 of Group 2 tumors were pathologically described as poorly differentiated, which suggests that this subtype is characterized by either the presence of fibroblasts and a strong desmoplastic response, and/or these tumors may have undergone an epithelial to mesenchymal transition.

The subtype of tumors identified by the pink dendrogram branch (Group 3) contained the three normal tonsillar epithelium samples and eleven tumors and was defined by the consistent expression of the Figure 1D pattern. Figure 1D contains the genes for Microsomal Glutathione S-Transferase 2, Cytokeratin 15 that identifies the basal cell layer of stratified squamous epithelia (Figure 2A; Lloyd et al., 1995), and Cytokeratin 4 that identifies the suprabasal layer of stratified squamous epithelia (Figure 2D; van der Velden et al., 1993). These three genes were recently identified in a microarray study on HNSCC progression and shown to be expressed at lower levels in HNSCC tumors versus normal epithelium (Ha et al., 2003), which is precisely what was observed here. Only 6 of the 47 tumors tested for Cytokeratin 15 expression by IHC were positive; however, 5 of these 6 tumors were in Group 3 (Figures 2I and 2J).

The subtype of tumors in the far right dendrogram branch (Group 4, green branch) showed high expression of the genes in Figure 1G, many of which are antioxidant-induced enzymes that are involved in xenobiotic metabolism including Glutathione S-Transferase M3, Thioredoxin Reductase 1, Glutathione Peroxidase 2, Aldo-Keto Reductase 1, and two genes involved in the pentose phosphate cycle (Transaldolase 1 and Phosphoglucuronate Dehydrogenase). These exact same six genes were recently shown by Hackett et al. (2003) to be more highly expressed in the epithelium of smokers than nonsmokers. These data suggest that either these tumors have a more dramatic and sustained response to cigarette smoke than the other three

groups, or that Group 4 subtype patients were current and active smokers.

To assess the significance of the overlaps between our data and the selected gene lists described from other studies, we performed a "simulation analysis" to determine the likelihood of finding this degree of gene overlap by chance (see Experimental Procedures). A simulation was performed by randomly selecting a set of genes from the entire set of 12,814. The number selected was set to the number of genes in our subset being tested. These randomly selected gene sets were then compared with the corresponding published gene set, the overlap determined, and then the entire process was repeated 10,000 times. In the final step, the actual number of overlapping genes between our lists and the published lists were compared to the simulated distributions. Using this analysis, we determined that the likelihood of obtaining the six gene overlap between the smoking-associated gene set of Hackett et al. (2003) and our intrinsic gene list was  $p < 0.01$ , and  $p < 0.0001$  if we use just the 21 genes present in Figure 1G (which we believe to be the most appropriate subset to base this calculation upon). We also performed a "simulation analysis" for the gene subset present in Figure 1D where we compared this subcluster to the "normal versus tumor" list from Ha et al. (2003), which gave  $p < 0.05$  for the entire intrinsic list and  $p < 0.0001$  if we use the subset in Figure 1D only.

We also profiled four HNSCC-derived cell lines with these data displayed to the left of the tumor-associated cluster diagram (Figure 1). The cell line data was included in a separate cluster analysis and was median centered using both the cell lines and tumors, while the tumor data presented in Figure 1 was median centered using only the tissue samples. This was done because the cell lines were very different in expression from the tissue samples, and by median centering the cell lines relative to the tumors, direct comparisons could be more readily made. When compared directly to the tumors, the cell lines did not show any of the dominant patterns of gene expression that were seen in the tumors, even though these lines were derived from primary HNSCC samples.

### Correlation of expression subtypes with clinical parameters

The median follow-up time on our HNSCC cohort was 16 months. Because of this relatively short follow-up, we used recurrence-free survival (RFS) as our primary endpoint where we define an "event" as the time to disease relapse or death. In our cohort, there were 18 patients who either died or had a recurrence. We first examined our intrinsic subtypes by univariate modeling for RFS using Cox regression analysis based upon the dendrogram branching pattern in Figure 1B; we first divided the samples into two subsets based upon the first major dendrogram branch, which combines Groups 2–4 into a single category versus Group 1 ( $p = 0.03$ ). The second logical grouping based upon the dendrogram has Group 1 and Group 2 as separate entities and combines Groups 3 and 4 in a single category ( $p = 0.017$ ). Finally, we examined each group separately ( $p = 0.02$  for the four groups). Figures 3A and 3B are Kaplan-Meier plots of RFS curves for the intrinsic subtypes; in Figure 3A we divided the samples into Group 1 versus Groups 2–4 as was done above (log rank  $p = 0.02$ ), and Figure 3B shows Group 1 versus Group 2 versus Groups 3 and 4, which gave a log rank  $p = 0.04$ .

Tumor subsite (hypopharynx versus other 3 sites,  $p = 0.01$ ),

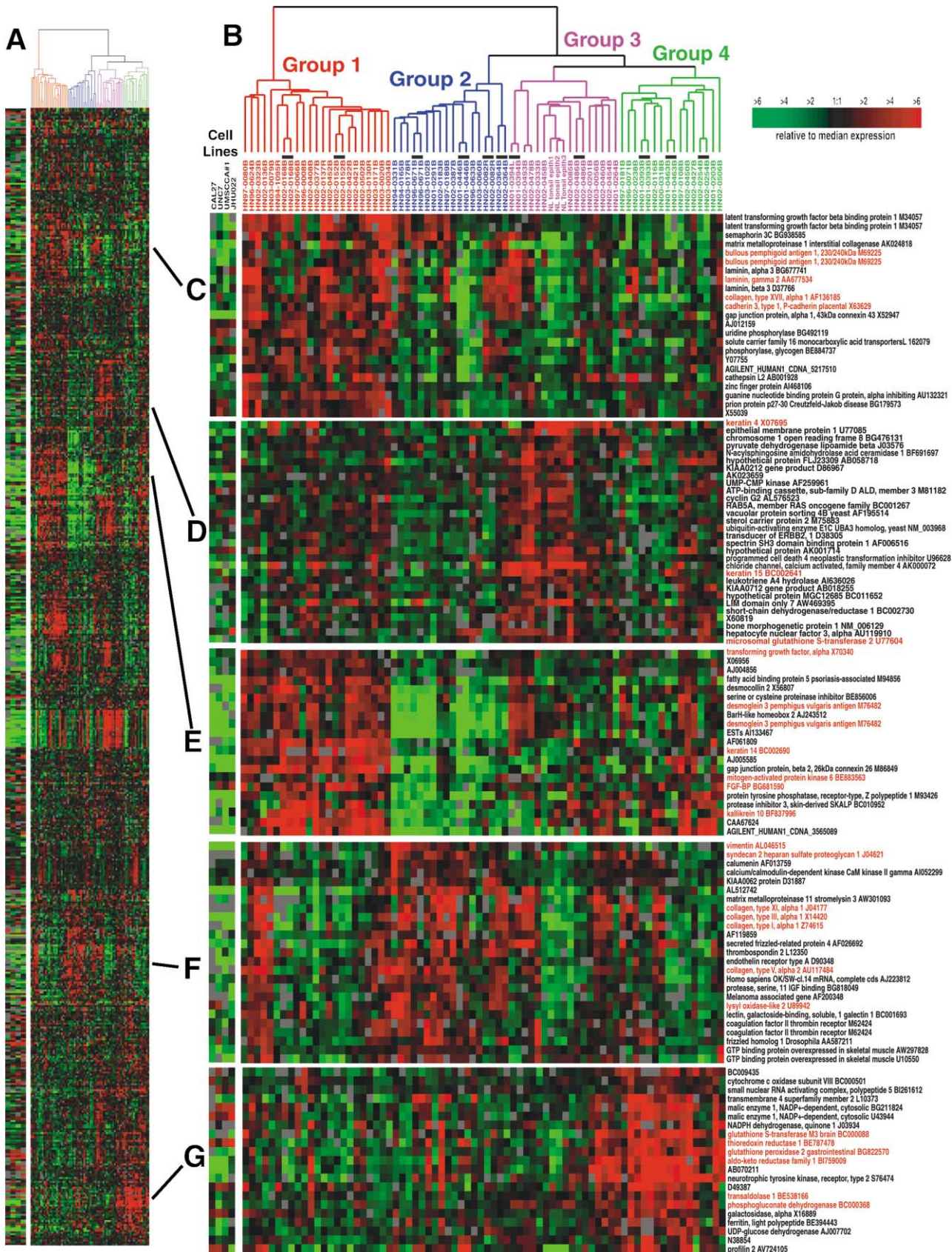


**Figure 1.** Intrinsic gene set cluster analysis of 60 HNSCC samples

An intrinsic analysis of 11 paired head and neck epithelial samples was performed and identified 582 cDNA clones that were analyzed using a two-way hierarchical clustering analysis.

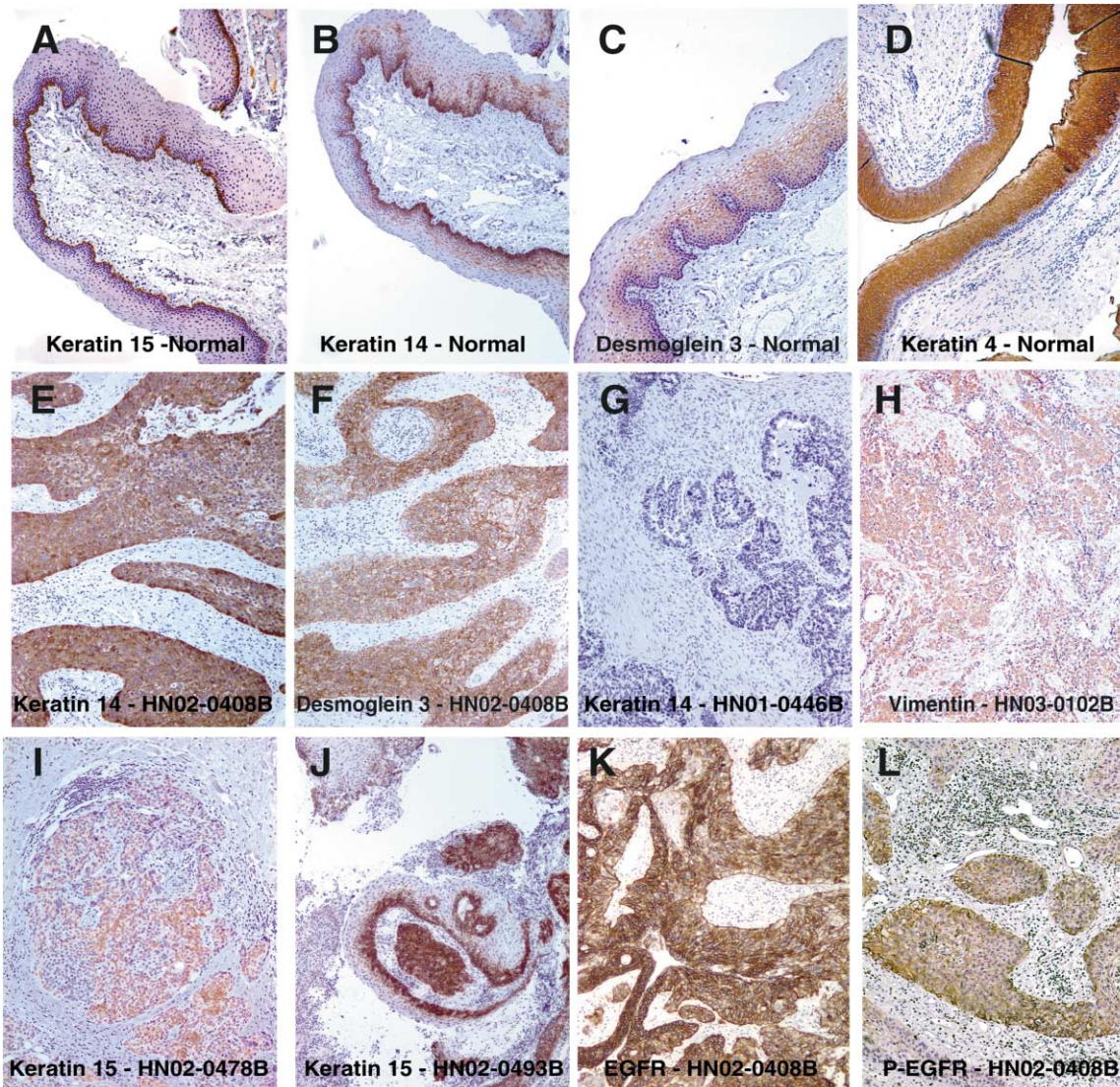


**Figure 2.** Immunohistochemical analysis of HNSCC samples

Normal tonsillar epithelium (A–D) and HNSCC samples (E–L) were analyzed by IHC for proteins from the intrinsic gene set and from the EGFR pathway.

**A:** Normal epithelium stained for Cytokeratin 15 showing basal layer staining.

**B:** Normal epithelium stained for Cytokeratin 14.

**C:** Normal epithelium stained for Desmoglein 3 showing plasma membrane staining.

**D:** Normal epithelium stained for Cytokeratin 4 showing suprabasal staining.

**E:** Tumor HN02-0408B (Group 1) stained for Cytokeratin 14.

**F:** Tumor HN02-0408B stained for Desmoglein 3.

**G:** Tumor HN01-0446B (Group 2) stained for Cytokeratin 14.

**H:** Tumor HN03-0102B (Group 2) stained for Vimentin.

**I:** Tumor HN02-0478B (Group 3) stained for Cytokeratin 15.

**J:** Tumor HN02-0493B (Group 3) stained for Cytokeratin 15.

**K:** Tumor HN02-0408B (Group 1) stained for EGFR.

**L:** Tumor HN02-0408B stained for the Tyr-1173 phosphorylated EGFR. Magnification for all images was 100×.

**Figure 1.** (continued)

**A:** Scaled-down version of the complete cluster diagram (also available as Supplemental Figure S1).

**B:** Close-up of the experimental sample-associated dendrogram with the intrinsic pair samples identified by the horizontal black lines. Each sample is color-coded according to its tumor subtype.

**C:** P-cadherin containing gene cluster.

**D:** Gene set containing Cytokeratin 15, which is enriched in normal tonsillar epithelium and Group 3 tumors.

**E:** Gene set containing TGF- $\alpha$  and Cytokeratin 14, enriched in Group 1 tumors.

**F:** Collagen-containing gene set present in Group 2 tumors.

**G:** Antioxidant and xenobiotic metabolism-related gene set. The genes in red represent genes discussed in the text.

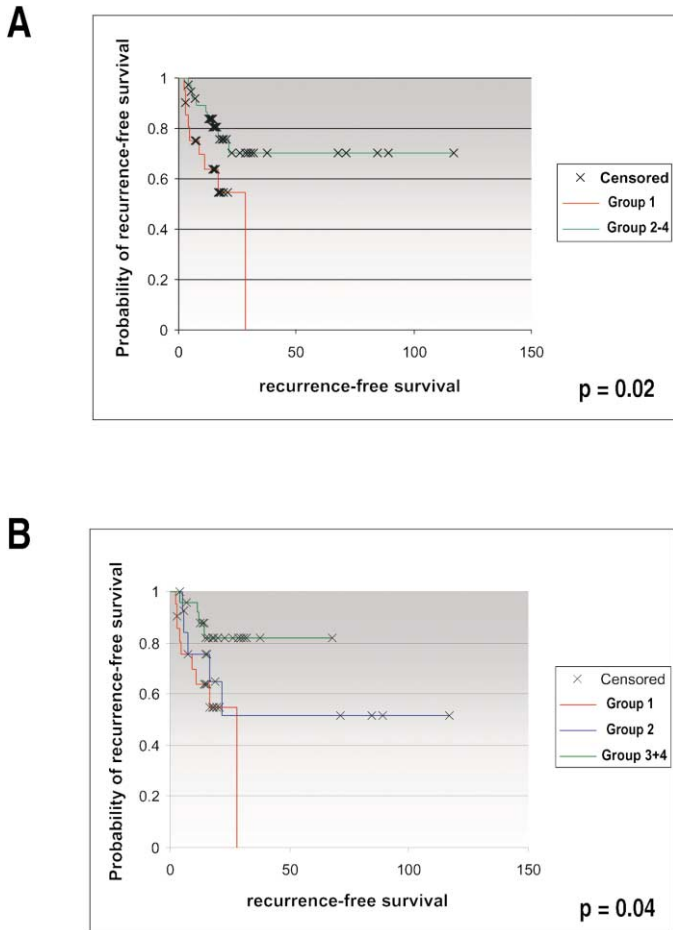


**Figure 3.** Kaplan-Meier survival analysis analyzed using a log-rank test

The samples were grouped according to the major dendrogram branches presented in Figure 1 and analyzed using recurrence-free survival as the endpoint (where an event is either a disease recurrence or death).

**A:** K-M analysis of Group 1 versus Groups 2–4 combined.

**B:** K-M analysis of Group 1 versus Group 2 versus Groups 3 and 4 combined.

age ( $p = 0.05$ ), and histological differentiation ( $p = 0.04$ ) were also prognostic factors when using Cox regression analysis and RFS as the endpoint; however, we did not find any significant associations between the clinical parameters and our intrinsic subtypes by way of contingency table analyses. We also examined what parameters would make the best bivariable model and determined that the top two models were (1) 3 intrinsic groups (Group 1 versus Group 2 versus Groups 3 and 4) and hypopharynx subsite ( $p = 0.03$  and  $p = 0.046$ , model chi-square = 10.04,  $p = 0.007$ ) and (2) 3 intrinsic groups and histological differentiation ( $p = 0.04$  and  $p = 0.01$ , model chi-square = 10.91,  $p = 0.004$ ). This finding is in agreement with the lack of correlation between our intrinsic classification and the clinical parameter. We also performed SAM (Tusher et al., 2001) supervised analyses to determine if any tumor subsite of origin showed distinctive expression features and found that no subsite showed a distinctive expression pattern (data not shown). Due to the small number of deaths in our cohort (15 deaths), the only parameters that were significant predictors of overall survival were tumor subsite (hypopharynx versus other

**Table 2.** Lymph node metastasis prediction accuracies

	PAM	KNN-Euclidean
Clinical LN; 55 tumors	58%; 159 genes	60%; 200 genes
Path LN; 38	60%; 2047 genes	57%; 100 genes
Clinical LN No OC; 40	53%; 55 genes	58%; 50 genes
Path LN No OC; 26 <sup>a</sup>	83%; 1548 genes	83%; 500 genes

<sup>a</sup>All analyses were conducted using a 10-fold cross validation analysis, except for the "Path LN No Oral Cavity" predictor, which was done using a leave 23% (6) out analysis

3 sites,  $p = 0.027$ ) and our 3-class intrinsic classification ( $p = 0.04$ ) when using Cox regression analysis and a cutoff of  $p < 0.05$  to determine statistical significance.

### Lymph node metastasis prediction

The presence or absence of lymph node metastases is one of the most important predictors of disease outcome in HNSCC patients (Andersen et al., 1994). All 55 of the primary tumors that we analyzed had known clinical lymph node (LN) metastasis status, and 38 also had pathological LN status (26 LN positive and 12 LN negative). The five tumors that were recurrence at the primary sites were excluded from these LN analyses. To develop a predictor for LN metastasis status, we utilized two different supervised statistical analyses. Our predictors included (1) a simple gene selection method coupled to sample predictions made using an Euclidian correlation to the K-Nearest Neighbors (KNN) of a given sample ( $K = 3$ ) (Dudoit et al., 2002) and (2) PAM analysis as described by Tibshirani et al. (2002). Starting with clinical LN status as the supervising parameter, we obtained a prediction accuracy of 60% (KNN) and 58% (PAM) when performing a 10-fold cross validation analysis (Table 2 and see Experimental Procedures). Because clinical LN status can differ when compared to pathological LN status, we also tested pathological LN status as the supervising parameter and obtained an accuracy of 57% (KNN) and 60% (PAM).

These low accuracies are likely due to the complex nature of metastasis, which is influenced by biological, temporal, and anatomical features. In particular, there is some evidence that the different subsites of HNSCC origins can contribute to clinical differences (Freier et al., 2003; Huang et al., 2002). Therefore, we examined the individual sample predictions made by our pathological metastasis predictors and noticed that 7/13 (KNN) and 6/13 (PAM) mistakes were made on the oral cavity-derived tumors. The observation that approximately half of the mistakes were made on a single subsite suggested that this subsite might be distinct from the others, or more heterogeneous, and therefore we removed the oral cavity-derived tumors from our analysis and trained a predictor using only the other three subsites (i.e., oropharynx, hypopharynx, and larynx). When using clinical node status (minus oral cavity) as supervision, we obtained an accuracy of 53% and 58%; however, when using pathological node status, we obtained an accuracy of 83%. These data suggest that even though there were no consistent expression differences that differentiated among the subsites, the oral cavity samples were different from the other three subsites or were more heterogeneous than the other subsites when it comes to expression patterns.

In order to visualize the transcriptional complexity of the

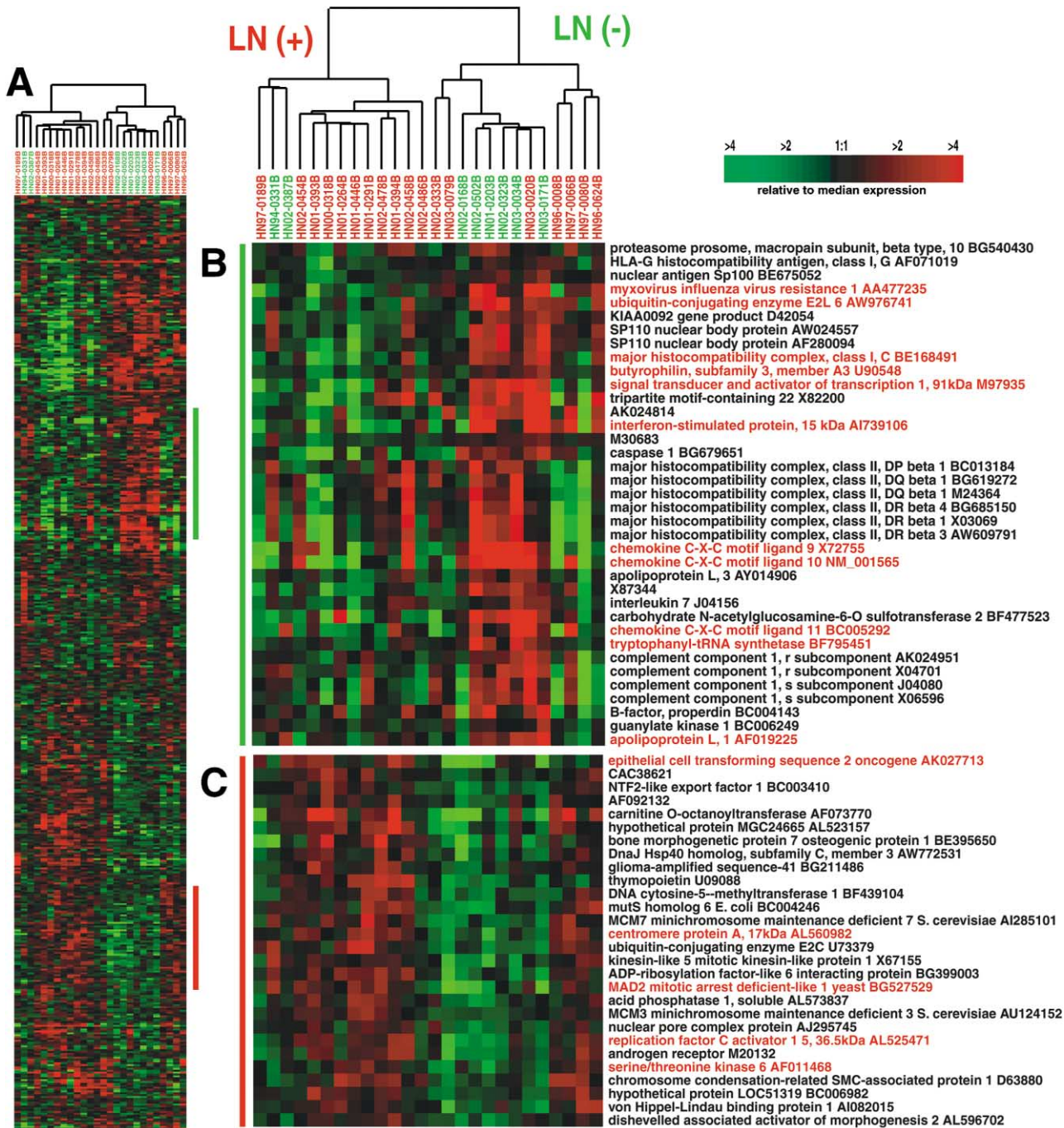


**Figure 4.** Hierarchical clustering analysis of the genes that were predictive of the presence or absence of lymph node metastases in HNSCC tumors

The 500 genes that were associated with prediction of pathological nodal status in HNSCC tumors derived from the larynx, hypopharynx, and oropharynx (no oral cavity tumors) were used in a two-way clustering analysis across the 26 samples. The node-negative samples are labeled in green and the node-positive samples are labeled in red.

**A:** Scaled-down version of the complete cluster diagram (also available as Supplemental Figure S2).

**B:** Close-up of the interferon-regulated gene set.

**C:** Close-up of the set of genes associated with cell proliferation rates.

metastasis prediction lists that were generated separately during each round of cross validation (CV), we compiled a list of the 500 genes that were the most frequently occurring across the 10 runs of the cross validation nodal predictors (see Experimental Procedures). We then used this gene set in a hierarchical

clustering analysis on the 26 tumors with pathological node status and that were not from the oral cavity (Figure 4 and Supplemental Figure S2 at <http://www.cancer.org/cgi/content/full/5/5/489/DC1>). This analysis sorted the samples into approximately four dendrogram branches and placed 6/8 of the LN(-)

samples into a common dendrogram branch; the two LN(-) samples that sorted to the left branch correspond to the two that were misclassified using our predictors. These six LN(-) samples were characterized by the high expression of many genes involved in immune functions (CXCL9, CXCL10, CXCL11, HLA-C) and interferon signaling (STAT1, MX1, and ISG15). Recent expression profiling studies of lymph node metastasis status in breast cancers also identified genes involved in immune and interferon functions as being predictive of metastasis status (Huang et al., 2003) and demonstrated that the 11 genes shown in red in Figure 4B were exactly shared between our study and the study of Huang et al. (2003); a "simulation analysis" showed that this degree of overlap is likely significant at the  $p < 0.0001$  level when using the gene subset present in Figure 4B as the basis for assessing overlap. Caspase 4 was also shared between these two studies, and the LN(-) HNSCC samples also showed high expression of Caspase 1. This surprising similarity across different data sets validates the findings of each study and suggest that immune cell function may play a role in the metastatic process.

As expected, there were also genes whose expression tended to be higher in the LN(+) tumors, especially the tumors contained within the dendrogram branch near the center that was entirely composed of LN(+) samples. Included in this gene set were STK6, RFC, MAD2, ECT2, and CENPA (Figure 4C); these five genes are of importance because they were present in the distant recurrence predictor of van't Veer et al. for breast cancer (van't Veer et al., 2002). In the van't Veer et al. and our study, the high expression of these genes was seen in the tumors that have metastases or that will go on to form distant metastases. Finally, some of the other genes in Figure 4C are known proliferation-associated genes including MCM3, MCM7, and Kinesin-like 5 (Perou et al., 1999, 2000; Sorlie et al., 2001).

## Discussion

Head and neck squamous cell carcinomas show significant heterogeneity in their clinical behavior that cannot presently be predicted using the current set of clinical markers; therefore, the development of new biomarkers for survival predictions would be valuable. Previous microarray-based studies of HNSCC have primarily focused on tumor versus normal patterns of expression (El-Naggar et al., 2002; Hwang et al., 2003; Leethanakul et al., 2003). Others have suggested that there might be subtypes of HNSCC (Belbin et al., 2002); however, to date no study has shown statistically significant differences in clinical outcomes between subtypes of HNSCC based upon gene expression patterns. Here we identified four distinct subtypes of HNSCC based upon an "intrinsic analysis" and showed that these subtypes had differences in recurrence-free survival and overall survival. These expression signatures are revealing of the complex biology that underlies HNSCC; however, these data will need to be confirmed by further research and by functional assays.

The tumor subtype with the worst outcome was the Group 1 tumors that were characterized by the high expression of TGF $\alpha$ , which is known to associate with poor clinical outcomes in HNSCC (Endo et al., 2000; Grandis, 1998; Quon et al., 2001). Most HNSCC tumors express EGFR (54/56 tested here were EGFR+ and see Figure 2K); however, there is additional evidence that suggests the Group 1 tumors have an activation of

the EGFR pathway. This evidence includes the genes contained within Figure 1E, which includes a major ligand of EGFR (TGF $\alpha$ ), a kinase that is in the downstream signaling cascade of EGFR (MKN6), and an angiogenic switch molecule induced by EGF (FGF-BP) (Harris et al., 2000). In addition, 15/19 of the Group 1 subtype tumors tested by IHC were positive for the Tyr-1173 phosphorylated form of the EGFR (Figure 2L), which has been used in the research settings as a marker for activation of EGFR (Heimberger et al., 2002). These data suggest that Group 1 patients should be evaluated for benefits from EGFR inhibitor-containing treatment regimens.

The expression profiling of breast tumors has also identified distinct tumor subtypes that predicted patient outcomes, with one of the most aggressive subtypes (basal-like) showing the high expression of Bullous Pemphigoid Antigen 1, P-Cadherin, Laminin  $\gamma$  2, and Collagen XVII- $\alpha$  (Sorlie et al., 2001, 2003), and with many of these same genes also being highly expressed in lung squamous carcinomas (Chung et al., 2002; Garber et al., 2001). The Group 1 subtype was also distinguished by the high expression of these four genes. In both breast and HNSCC, tumors showing the high expression of these four genes showed poor patient outcomes. These data suggest that either these genes are causative of poor outcomes or they are expressed by a distinct cell type(s) that consistently gives rise to aggressive tumors.

The other three HNSCC subtypes also showed distinct expression profiles, some of which have been seen in complementary airway epithelial microarray studies. The Group 2 tumors showed a strong mesenchymal cell signature due to the presence of many fibroblasts and a lack of epithelial expression-based differentiation features, and some may have even undergone an epithelial to mesenchymal transition (Figures 1F, 2G, and 2H). The Group 3 tumors contained the normal tonsil epithelium samples and corroborated the normal versus HNSCC study of Ha et al. (2003). The Group 3 tumors were also almost exclusively the only Cytokeratin 15-positive tumors as assayed by IHC (5/6 CK15-positive tumors were in this subtype). It is interesting to note that the protein expression patterns of Cytokeratins 14 and 15 were similar in normal tonsillar epithelial samples (Figures 2A and 2B) but were quite distinct in HNSCC tumors, with most (41/47) HNSCCs being positive for Cytokeratin 14 and only a handful (6/47) being positive for Cytokeratin 15. In addition, the Group 3 tumors showed the fewest patient RFS events (one), which is similar to what was seen in lung carcinomas where the group of tumors that clustered nearest the normal lung samples showed the best outcomes (Garber et al., 2001).

The Group 4 tumors showed an expression pattern that was very similar to the pattern of gene expression induced by exposure to cigarette smoke (Hackett et al., 2003). These data suggest that the Group 4 tumors either have a sustained response to cigarette smoke or that patients in the Group 4 subtype are current smokers. The majority of our cohort has a heavy smoking history (all but two were smokers); however, the time from the last cigarette smoke exposure to the time of tissue collection was not available so we cannot determine if this is an acute or sustained response pattern. In addition, these data suggest that there could be variations within smokers in the ability to respond to cigarette smoke. Finally, we also profiled four primary HNSCC-derived cell lines and saw that none of these cell lines showed the dominant patterns of expression that defined the tumor subtypes. This finding is similar to our

earlier comparisons of breast tumors to breast cell lines where significant differences between cell lines and tumors were observed (Ross and Perou, 2001).

There have been a few studies to suggest that metastases show similar profiles to the primary tumors that they arose from (Garber et al., 2001; Perou et al., 2000), suggesting that the biological properties of a primary tumor can reflect the properties of its metastases (Ramaswamy et al., 2003). To take this one step farther, some have shown that the presence of metastases at the time of surgery can be predicted based upon gene expression patterns present in the primary tumor (Huang et al., 2003). The accuracy of our HNSCC “metastasis predictor” when using pathologically determined nodal status was approximately 60%, but was improved to 83% when one of the four tumor subsites was removed from the analysis (oral cavity). Our findings support the hypothesis that lymph node metastasis status can be predicted using the gene expression patterns of the primary tumor. Our pathological node status predictor gene set also showed significant similarities with other microarray analyses of the metastatic processes in breast tumors. Namely, we identified a likely STAT1-regulated gene cluster (Darnell, 1997; Lehtonen et al., 1997; Perou et al., 1999) as being useful in predicting lymph node metastasis status, as did the study of Huang et al. (2003), and we identified a “proliferation” signature that shared many genes with the distant recurrence predictor of van 't Veer et al. (2002). These similarities in which the high expression of identical genes are predicting similar behaviors across HNSCC tumors and two breast tumor data sets identifies common pathways and/or genes that could be playing similar roles in epithelial tumor metastasis.

In summary, this work has identified a number of important biological differences among HNSCC samples that could have an impact upon clinical treatment regimens and patient outcomes if these patterns are validated on additional cohorts. In particular, we identified discriminatory patterns of expression in our HNSCC tumors that were previously seen in microarray analyses of epithelial tumors of the breast and lung (Garber et al., 2001; Huang et al., 2003; Perou et al., 1999, 2000; Sorlie et al., 2001; van 't Veer et al., 2002), in airway tissue and tumor studies (Ha et al., 2003; Hackett et al., 2003), and a pattern associated with activation of the EGFR pathway. The agreement between our study and these other studies done on HNSCC and different tumor sites (and done on different microarray platforms) validates the biological insights obtained here. This study, therefore, can serve as a central point to tie all of these studies together into a common framework and has added new patterns and complexities. The patterns identified here should be evaluated on new and independent cohorts, and if confirmed, will represent an important new set of biomarkers for HNSCC prognostication and prediction of clinical outcomes.

## Experimental procedures

### Patient biopsy samples and the common reference sample for array hybridization

Sixty fresh frozen HNSCC samples were obtained from the University of North Carolina at Chapel Hill (UNC) Tissue Procurement Core Facility from patients undergoing surgery at the UNC Hospital and who consented to have their tumor tissue used for cancer research using an Institutional Review Board approved protocol. Fifty-five tumor samples were collected from the primary tumor (labeled B in Figure 1), and five tumor samples were collected from a local recurrence at the primary tumor site (labeled R in Figure 1). For

one primary tumor, an associated lymph node metastasis was also available (labeled L in Figure 1). Patient clinical information can be found in Supplemental Table S1 (<http://www.cancercell.org/cgi/content/full/5/5/489/DC1>) and patient demographics are presented in Table 1. These patients were heterogeneously treated in accordance with the standard of care dictated by their disease stage. Staging and treatment planning were determined by consensus of the UNC Head and Neck Tumor Board. Clinical staging (55 tumors) of the neck was determined by clinical exam and contrasted CT or MRI imaging, while pathologic staging (38 tumors) was determined by routine H&E staining of neck nodes in patients undergoing a neck dissection.

We also profiled three normal tonsillar epithelium samples that were collected from three pediatric patients following routine tonsillectomy and four HNSCC primary tumor-derived cell lines (UNC7, UMSCCA1, CAL27, and JHU022). Each experimental sample (tumor, normal, or cell line) was assayed versus a common reference sample consisting of a pool of total RNA derived from a randomly chosen subset of 30 of the HNSCC samples. This tumor pool reference strategy has been successfully used in another profiling study (van 't Veer et al., 2002). In total, 78 experiments were performed using three separate preparations of the common reference pool.

### RNA preparations, labeling, and microarray hybridizations

Total RNA was purified from each sample using the Qiagen RNeasy Midi Kit according to the manufacturer's protocol (Qiagen, Valencia, CA) and 25–50 milligram of tissue per sample. The integrity of the RNA was determined using the RNA 6000 Nano LabChip Kit and an Agilent 2100 Bioanalyzer (Agilent Technologies, Palo Alto, CA). Ten micrograms of total RNA were amplified per sample, using an Arcturus RiboAmp RNA Amplification kit (Arcturus, Mountain View, CA) with the following modifications. Amino-allyl-UTP (aa-UTP) was used in the *in vitro* transcription step to perform an “indirect” labeling of the amplified RNA (aRNA). Rather than using the supplied IVT Master Mix as provided, we added aa-UTP into the IVT NTP mix at a ratio of aa-UTP:UTP of 4:1. For indirect labeling of aRNA, 10  $\mu$ g of the common reference amplified RNA (aRNA) was labeled with a Cy3 Monofunctional Reactive Dye (Amersham Biosciences, UK) and 10  $\mu$ g of aRNA from each experimental sample was labeled using a Cy5 Monofunctional Reactive Dye. The dye was quenched with 4 M hydroxylamine (Sigma, St. Louis, MO) after a 1 hr incubation and unincorporated dye molecules were removed using a Qia-Quick PCR Purification Kit.

The labeled common reference and individual experimental samples were combined along with 20  $\mu$ g of COT-1 DNA (GIBCO-BRL), 20  $\mu$ g of polyA DNA, and 20  $\mu$ g of yeast tRNA and hybridized to a 12,814 gene Agilent Human 1 cDNA microarray (Agilent Technologies). The reaction mix was hybridized on the array overnight at 65°C in 3 $\times$  SSC. The microarrays were then washed using 2 $\times$  SSC/0.025% SDS, followed by 1 $\times$  SSC, and finally a 0.2 $\times$  SSC wash. Washed arrays were quickly scanned on an Axon 4000B Scanner. Image analysis was accomplished using GenePix Pro 4.0. The raw data (.gpr files) tables were uploaded into the UNC Microarray Database, which is a mirror of the Stanford Microarray Database (Sherlock et al., 2001). A global, linear normalization was performed to adjust the Cy3 and Cy5 channels (Sherlock et al., 2001). All microarray raw data tables are available at the UNC Microarray Database (<https://genome.unc.edu/>), at the supporting website for this paper (<http://dragon.med.unc.edu/pubsup/HN/>), and in the Gene Expression Omnibus under the accession number of GSE686 (submitter C. Perou).

### Statistical analysis of microarray data

#### Intrinsic gene set analysis

The background subtracted, normalized log<sub>2</sub> ratio of red over green intensity values were first filtered to select genes that had a signal intensity of at least 1.5-fold above background in both the Cy5 and Cy3 channels. Only genes that met these criteria in at least 80% of the 60 tissue samples were included for subsequent analysis. Next, we corrected for the systematic bias that may have been introduced by using different batches of the common reference before further statistical analyses. We used “Distance Weighted Discrimination/DWD” as described in Benito et al. (2004) on the two largest sets of samples assayed using two different batches of common reference (one reference batch used only eight samples, which is too few to perform the correction). Next, we performed an intrinsic analysis as described in Sorlie et al. (2003) by assaying spatially distinct pieces of the same tumor. We used ten tumor pairs that were separate pieces and RNA preparations

of the same tumor, one tumor pair that was a tumor and its lymph node metastasis, and designated two of the three normal tonsillar epithelia samples as a pair. Using this sample set, we searched for genes that were the least variable within pairs and that were variable across different samples by computing for each gene the average "within-pair variance" (the average of the variance within each tumor pair) and the "between-subject variance" (the average of the variance across all pairs not assessed for within pair variance). We then computed the ratio  $D = (\text{within-pair variance})/(\text{between-subject variance})$  and declared those genes with the smallest values of  $D$  to be intrinsic. The choice of a  $D$  value cutoff was set at one standard deviation below the average (using the "Intrinsic Gene Identifier v1.0" by Max Diehn/Stanford University). This analysis resulted in the selection of 582 clones representing 547 genes. We finally used these 582 clones to perform a two-way average linkage hierarchical cluster analysis using the program "Cluster" (Eisen et al., 1998) with the data being displayed relative to the median expression for each gene (i.e., median centering of the rows). The cluster results were then visualized using "TreeView."

#### Supervised microarray analyses

To investigate relationships between gene expression patterns and patient-associated parameters, we performed supervised analyses to identify gene sets that correlated with clinical parameters and then tested the ability of these sets to make reliable predictions (Huang et al., 2003). In each case, we utilized two different statistical methods to train a gene expression predictor for a single parameter (e.g., lymph node metastasis status). These methods included a K-Nearest Neighbor (KNN) metric that uses a Euclidian correlation coefficient to determine the distance of a sample to its three nearest sample neighbors (Dudoit et al., 2002) and Prediction Analysis of Microarray (PAM) (Tibshirani et al., 2002). To select genes for the K-Nearest Neighbor method, we used our own version of a gene selection method that was first described by Dudoit et al. (2002); the KNN genes were identified in the training set according to the ratio of between-group to within-group sums of squares (Dudoit et al., 2002). The top  $n$  ranked genes were used during each round of cross validation. The size of the gene subset was increased for subsequent rounds of CV. The set of  $n$  top-ranked genes that gave the highest average prediction accuracy during CV was also determined and reported. Gene selection for PAM was completed as described in Tibshirani et al. (2002).

For all but one nodal predictor, we performed a 10-fold cross validation (CV) analysis to iteratively optimize the list of genes and to determine prediction accuracies. Each round of CV would begin by splitting the samples into a training set (90% of the samples) and a test set (10% left-out samples), with gene selection and training being performed on the 90% and then used to predict the status of the withheld 10%. This was repeated 10 times, each time using a different 10% subset and a different gene set. Our reported prediction accuracies are the average of these iterative cycles of prediction. The one parameter that had a different test was pathological node status trained on just the three tumor subsites (oropharynx, hypopharynx, and larynx with the oral cavity samples not included); due to the importance of this predictor, we performed a 23% cross validation analysis where 6 of the 26 samples were withheld, and then a predictor was trained on the 20 samples and applied to the 6 samples. This was repeated 10 times with our reported prediction accuracies reflecting the average of the predictions made onto the withheld 60 samples. The genes presented in Figure 4 and Supplemental Figure S2 (<http://www.cancer.org/cgi/content/full/5/5/489/DC1>) are a statistical tabulation of the list of genes that predicted pathological nodal status in the three subsites (no oral cavity); to derive this list, we compared each of the 10 lists generated in each round of the 23% cross validation analysis and saved the score for each gene during each round. We then summed the scores for each gene across all rounds and sorted this list to get the top 500 (this list was not used for any predictions but was used for the cluster analysis).

#### Statistical analysis of clinical correlates

Cox regression was used to examine the impact of covariates (intrinsic subtypes, age, sex, ethnicity, tumor subsite, clinical stage, and LN status) on three different endpoints. These endpoints were: (1) time to disease recurrence (or progression), (2) recurrence-free survival (defined here as the time to disease recurrence or death), and (3) overall survival (defined as time to death). The Kaplan-Meier (or product limit) method was used to estimate these survivorship-type functions. We also used Fisher's exact test for data categorized into two by two contingency tables. Nonparametric one-way

analysis of variance or Wilcoxon rank-sum tests (using normal scores) were used on continuous variables to evaluate the possible difference in response across the two (or more) categories. These statistical analyses were performed using SAS statistical software, Version 8.2, SAS Institute Inc. (Cary, NC).

#### Simulation analysis

The simulation was performed by randomly selecting a set of genes from the entire set of 12,814. The number randomly selected was set to the number of genes in our subset being tested. This randomly selected set was then compared for overlap, with the corresponding gene sets that were mentioned from published studies. The number of genes found in the overlap was recorded and the process was repeated 10,000 times. In the final step, the actual amount of overlap was compared between our gene sets and the published gene sets, and this was compared to the simulated distribution. This comparison gives the likelihood of finding co-occurrences by chance. The simulation was performed independently for each of the three gene sets thought to have a significant overlap.

#### Immunohistochemistry

Formalin-fixed and paraffin-embedded tissue blocks from (at most) 56 tumors were available for immunohistochemistry (IHC) staining. 5  $\mu\text{m}$  tissue sections were deparaffined with xylene and dehydrated with sequential washes of 100%, 95%, and 70% ethanol, and endogenous peroxidase activity was blocked with a 3% hydrogen peroxidase solution. For EGFR IHC, the tissues were digested with Proteinase K and then incubated with a rabbit polyclonal antibody against the epidermal growth factor receptor (EGFR) using the DAKO EGFR PharmDx kit at the recommended antibody dilution (K1494, Carpinteria, CA). The sections were next incubated with polymer labeled HRP-goat anti-mouse antibody. For other antibodies, the samples were digested with Proteinase K and then steamed for antigen retrieval with citrate buffer (pH 7.0) for 30 min. The antibodies used included Cytokeratin 15 (1:100 dilution, LHK15, Novocastra Laboratory Ltd, UK), Cytokeratin 4 (1:200, 6B10, Novocastra), Cytokeratin 14 (1:500, MS-115-P1, NeoMarkers, Fremont, CA), Desmoglein 3 (1:30, 32-6300, Zymed Laboratories, CA), phosphorylated-EGFR-Tyr1173 (1:200, 44-794, Biosource, Camarillo, CA), and Vimentin (1:50, 18-0052, Zymed). These sections were next incubated with biotin-conjugated goat anti-mouse IgG (Vector Laboratories) and then streptavidin-conjugated HRP followed by the development of HRP activity using the ABC kit and substrate (Vector Laboratories). The slides were finally counterstained with 50% hematoxylin and examined by light microscopy on a Leica microscope at 100 $\times$  magnification. A three-point scoring system was used where 0 = invasive tumor cells present in the sample and no staining seen; 1 = invasive tumor cells present and weak intensity staining and/or <20% of cells stained; and 2 = invasive tumor cells present with strong staining in >20% of cells.

#### Acknowledgments

We wish to thank Phillip Bernard, Lucile Adams-Campbell, and Andy Olshan for reviewing this manuscript. This grant was supported by funds from the NCI Breast SPORE grant to UNC-CH (P50-CA58223-09A1 to C.M.P.), a Clinical/Translational Research Award by the Lineberger Comprehensive Cancer Center (C.H.C.), and funds from the American College of Surgeons Oncology Group (W.G.Y.). We also wish to acknowledge the technical assistance and support of the UNC-CH Tissue Procurement and Analysis Facility (supported by NCI grant P3916086-25), David Cowan for assistance with the IHC, Evangeline Reynolds for assistance with sample collection, and Sylvia Wrenn for collecting the clinical information.

Received: November 4, 2003

Revised: February 2, 2004

Accepted: March 9, 2004

Published: May 17, 2004

#### References

Alizadeh, A.A., Eisen, M.B., Davis, R.E., Ma, C., Lossos, I.S., Rosenwald, A., Boldrick, J.C., Sabet, H., Tran, T., Yu, X., et al. (2000). Distinct types of

- diffuse large B-cell lymphoma identified by gene expression profiling. *Nature* 403, 503–511.
- Andersen, P.E.M., Shah, J.P.M.F., Cambronero, E.M., and Spiro, R.H.M. (1994). The role of comprehensive neck dissection with preservation of the spinal accessory nerve in the clinically positive neck. *Am. J. Surg.* 168, 499–502.
- Belbin, T.J., Singh, B., Barber, I., Socci, N., Wenig, B., Smith, R., Prystowsky, M.B., and Childs, G. (2002). Molecular classification of head and neck squamous cell carcinoma using cDNA microarrays. *Cancer Res.* 62, 1184–1190.
- Benito, M., Parker, J., Du, Q., Wu, J., Xiang, D., Perou, C.M., and Marron, J.S. (2004). Adjustment of systematic microarray data biases. *Bioinformatics* 20, 105–114.
- Bhattacharjee, A., Richards, W.G., Staunton, J., Li, C., Monti, S., Vasa, P., Ladd, C., Beheshti, J., Bueno, R., Gillette, M., et al. (2001). Classification of human lung carcinomas by mRNA expression profiling reveals distinct adenocarcinoma subclasses. *Proc. Natl. Acad. Sci. USA* 98, 13790–13795.
- Chung, C.H., Bernard, P.S., and Perou, C.M. (2002). Molecular portraits and the family tree of cancer. *Nat. Genet.* 32 (Suppl), 533–540.
- Darnell, J.E., Jr. (1997). STATs and gene regulation. *Science* 277, 1630–1635.
- Dhanasekaran, S.M., Barrette, T.R., Ghosh, D., Shah, R., Varambally, S., Kurachi, K., Pienta, K.J., Rubin, M.A., and Chinnaiyan, A.M. (2001). Delineation of prognostic biomarkers in prostate cancer. *Nature* 412, 822–826.
- Dudoit, S., Fridlyand, J., and Speed, T.P. (2002). Comparison of discrimination methods for the classification of tumors using gene expression data. *J. Am. Stat. Assoc.* 97, 77–87.
- Edelman, D.B., Meech, R., and Jones, F.S. (2000). The homeodomain protein Barx2 contains activator and repressor domains and interacts with members of the CREB family. *J. Biol. Chem.* 275, 21737–21745.
- Eisen, M.B., Spellman, P.T., Brown, P.O., and Botstein, D. (1998). Cluster analysis and display of genome-wide expression patterns. *Proc. Natl. Acad. Sci. USA* 95, 14863–14868.
- El-Naggar, A.K., Kim, H.W., Clayman, G.L., Coombes, M.M., Le, B., Lai, S., Zhan, F., Luna, M.A., Hong, W.K., and Lee, J.J. (2002). Differential expression profiling of head and neck squamous carcinoma: significance in their phenotypic and biological classification. *Oncogene* 21, 8206–8219.
- Endo, S., Zeng, Q., Burke, N.A., He, Y., Melhem, M.F., Watkins, S.F., Lango, M.N., Drenning, S.D., Huang, L., and Rubin Grandis, J. (2000). TGF- $\alpha$  antisense gene therapy inhibits head and neck squamous cell carcinoma growth in vivo. *Gene Ther.* 7, 1906–1914.
- Freier, K., Joos, S., Flechtenmacher, C., Devens, F., Benner, A., Bosch, F.X., Lichter, P., and Hofele, C. (2003). Tissue microarray analysis reveals site-specific prevalence of oncogene amplifications in head and neck squamous cell carcinoma. *Cancer Res.* 63, 1179–1182.
- Garber, M.E., Troyanskaya, O.G., Schluens, K., Petersen, S., Thaesler, Z., Pacyna-Gengelbach, M., van de Rijn, M., Rosen, G.D., Perou, C.M., Whyte, R.I., et al. (2001). Diversity of gene expression in adenocarcinoma of the lung. *Proc. Natl. Acad. Sci. USA* 98, 13784–13789.
- Grandis, J.R. (1998). Levels of TGF- $\alpha$  and EGFR protein in head and neck squamous cell carcinoma and patient survival. *J. Natl. Cancer Inst.* 90, 824–832.
- Ha, P.K., Benoit, N.E., Yochem, R., Sciubba, J., Zahurak, M., Sidransky, D., Pevsner, J., Westra, W.H., and Califano, J. (2003). A transcriptional progression model for head and neck cancer. *Clin. Cancer Res.* 9, 3058–3064.
- Hackett, N.R., Heguy, A., Harvey, B.G., O'Connor, T.P., Luettich, K., Flieder, D.B., Kaplan, R., and Crystal, R.G. (2003). Variability of antioxidant-related gene expression in the airway epithelium of cigarette smokers. *Am. J. Respir. Cell Mol. Biol.* 29, 331–343.
- Harris, V.K., Coticchia, C.M., Kagan, B.L., Ahmad, S., Wellstein, A., and Riegel, A.T. (2000). Induction of the angiogenic modulator fibroblast growth factor-binding protein by epidermal growth factor is mediated through both MEK/ERK and p38 signal transduction pathways. *J. Biol. Chem.* 275, 10802–10811.
- Heimberger, A.B., Learn, C.A., Archer, G.E., McLendon, R.E., Chewing, T.A., Tuck, F.L., Pracyk, J.B., Friedman, A.H., Friedman, H.S., Bigner, D.D., and Sampson, J.H. (2002). Brain tumors in mice are susceptible to blockade of epidermal growth factor receptor (EGFR) with the oral, specific, EGFR-tyrosine kinase inhibitor ZD1839 (iressa). *Clin. Cancer Res.* 8, 3496–3502.
- Huang, Q., Yu, G.P., McCormick, S.A., Mo, J., Datta, B., Mahimkar, M., Lazarus, P., Schaffer, A.A., Desper, R., and Schantz, S.P. (2002). Genetic differences detected by comparative genomic hybridization in head and neck squamous cell carcinomas from different tumor sites: construction of oncogenetic trees for tumor progression. *Genes Chromosomes Cancer* 34, 224–233.
- Huang, E., Cheng, S.H., Dressman, H., Pittman, J., Tsou, M.H., Horng, C.F., Bild, A., Iversen, E.S., Liao, M., Chen, C.M., et al. (2003). Gene expression predictors of breast cancer outcomes. *Lancet* 361, 1590–1596.
- Hwang, D., Alevizos, I., Schmitt, W.A., Misra, J., Ohyama, H., Todd, R., Mahadevappa, M., Warrington, J.A., Stephanopoulos, G., and Wong, D.T. (2003). Genomic dissection for characterization of cancerous oral epithelium tissues using transcription profiling. *Oral Oncol.* 39, 259–268.
- Jemal, A., Thomas, A., Murray, T., and Thun, M. (2002). Cancer statistics, 2002. *CA Cancer J. Clin.* 52, 23–47.
- Jones, K.R., Lodge-Rigal, R.D., Reddick, R.L., Tudor, G.E., and Shockley, W.W. (1992). Prognostic factors in the recurrence of stage I and II squamous cell cancer of the oral cavity. *Arch. Otolaryngol. Head Neck Surg.* 118, 483–485.
- Landis, S.H., Murray, T., Bolden, S., and Wingo, P.A. (1999). Cancer statistics. *CA Cancer J. Clin.* 49, 8–31.
- Leethanakul, C., Knezevic, V., Patel, V., Amornphimoltham, P., Gillespie, J., Shillitoe, E.J., Emko, P., Park, M.H., Emmert-Buck, M.R., Strausberg, R.L., et al. (2003). Gene discovery in oral squamous cell carcinoma through the head and neck cancer genome anatomy project: confirmation by microarray analysis. *Oral Oncol.* 39, 248–258.
- Lehtonen, A., Matikainen, S., and Julkunen, I. (1997). Interferons up-regulate STAT1, STAT2, and IRF family transcription factor gene expression in human peripheral blood mononuclear cells and macrophages. *J. Immunol.* 159, 794–803.
- Lloyd, C., Yu, Q.C., Cheng, J., Turksen, K., Degenstein, L., Hutton, E., and Fuchs, E. (1995). The basal keratin network of stratified squamous epithelia: defining K15 function in the absence of K14. *J. Cell Biol.* 129, 1329–1344.
- MacDonald, T.J., Brown, K.M., LaFleur, B., Peterson, K., Lawlor, C., Chen, Y., Packer, R.J., Cogen, P., and Stephan, D.A. (2001). Expression profiling of medulloblastoma: PDGFRA and the RAS/MAPK pathway as therapeutic targets for metastatic disease. *Nat. Genet.* 29, 143–152.
- Perou, C.M., Jeffrey, S.S., van de Rijn, M., Rees, C.A., Eisen, M.B., Ross, D.T., Pergamenschikov, A., Williams, C.F., Zhu, S.X., Lee, J.C., et al. (1999). Distinctive gene expression patterns in human mammary epithelial cells and breast cancers. *Proc. Natl. Acad. Sci. USA* 96, 9212–9217.
- Perou, C.M., Sorlie, T., Eisen, M.B., van de Rijn, M., Jeffrey, S.S., Rees, C.A., Pollack, J.R., Ross, D.T., Johnsen, H., Akslen, L.A., et al. (2000). Molecular portraits of human breast tumours. *Nature* 406, 747–752.
- Quon, H., Liu, F.F., and Cummings, B.J. (2001). Potential molecular prognostic markers in head and neck squamous cell carcinomas. *Head Neck* 23, 147–159.
- Ramaswamy, S., Tamayo, P., Rifkin, R., Mukherjee, S., Yeang, C.H., Angelo, M., Ladd, C., Reich, M., Latulippe, E., Mesirov, J.P., et al. (2001). Multiclass cancer diagnosis using tumor gene expression signatures. *Proc. Natl. Acad. Sci. USA* 98, 15149–15154.
- Ramaswamy, S., Ross, K.N., Lander, E.S., and Golub, T.R. (2003). A molecular signature of metastasis in primary solid tumors. *Nat. Genet.* 33, 49–54.
- Ross, D.T., and Perou, C.M. (2001). A comparison of gene expression signatures from breast tumors and breast tissue derived cell lines. *Dis. Markers* 17, 99–109.
- Sessions, D.G., Spector, G.J., Lenox, J., Haughey, B., Chao, C., and Marks, J. (2002). Analysis of treatment results for oral tongue cancer. *Laryngoscope* 112, 616–625.

Sherlock, G., Hernandez-Boussard, T., Kasarskis, A., Binkley, G., Matese, J.C., Dwight, S.S., Kaloper, M., Weng, S., Jin, H., Ball, C.A., et al. (2001). The stanford microarray database. *Nucleic Acids Res.* 29, 152–155.

Sorlie, T., Perou, C.M., Tibshirani, R., Aas, T., Geisler, S., Johnsen, H., Hastie, T., Eisen, M.B., van de Rijn, M., Jeffrey, S.S., et al. (2001). Gene expression patterns of breast carcinomas distinguish tumor subclasses with clinical implications. *Proc. Natl. Acad. Sci. USA* 98, 10869–10874.

Sorlie, T., Tibshirani, R., Parker, J., Hastie, T., Marron, J.S., Nobel, A., Deng, S., Johnsen, H., Pesich, R., Geisler, S., et al. (2003). Repeated observation of breast tumor subtypes in independent gene expression data sets. *Proc. Natl. Acad. Sci. USA* 100, 8418–8423.

Takes, R.P., Baatenburg de Jong, R.J., Schuurung, E., Hermans, J., Vis, A.A., Litvinov, S.V., and van Krieken, J.H. (1997). Markers for assessment of nodal

metastasis in laryngeal carcinoma. *Arch. Otolaryngol. Head Neck Surg.* 123, 412–419.

Tibshirani, R., Hastie, T., Narasimhan, B., and Chu, G. (2002). Diagnosis of multiple cancer types by shrunken centroids of gene expression. *Proc. Natl. Acad. Sci. USA* 99, 6567–6572.

Tusher, V., Tibshirani, R., and Chu, G. (2001). Significance analysis of microarrays applied to the ionizing radiation response. *Proc. Natl. Acad. Sci. USA* 98, 5116–5121.

van der Velden, L.A., Schaafsma, H.E., Manni, J.J., Ramaekers, F.C., and Kuijpers, W. (1993). Cytokeratin expression in normal and (pre)malignant head and neck epithelia: an overview. *Head Neck* 15, 133–146.

van 't Veer, L.J., Dai, H., van de Vijver, M.J., He, Y.D., Hart, A.A., Mao, M., Peterse, H.L., van der Kooy, K., Marton, M.J., Witteveen, A.T., et al. (2002). Gene expression profiling predicts clinical outcome of breast cancer. *Nature* 415, 530–536.